Thieno[3,2-*b*]thiophene Flanked Isoindigo Polymers for High Performance Ambipolar OFET Applications

Iain Meager, Mark Nikolka, Bob C. Schroeder, Christian B. Nielsen, Miquel Planells, Hugo Bronstein, Joseph W. Rumer, David Ian James, Raja Shahid Ashraf, Aditya Sadhanala, Pascal Hayoz, Jean-Charles Flores, Henning Sirringhaus, and Iain McCulloch*

The synthesis of a new thieno[3,2-*b*]thiophene isoindigo (iITT) based monomer unit, and its subsequent incorporation into a series of alternating copolymers is reported. Copolymerisation with benzothiadiazole, bithiophene and thiophene comonomer units by palladium catalysed cross coupling gives three new narrow band gap semiconducting polymers for OFET applications. Extending the fused nature of the isoindigo core serves to further enhance molecular orbital overlap along the polymer backbones and facilitate good charge transport characteristics thus demonstrating the potential of extending the fused ring system that is attached to the isoindigo core. When used as the semiconducting channel in top-gate/bottom-contact OFET devices, good ambipolar properties are observed, with hole and electron mobilities up to 0.4 cm^2/Vs and 0.7 cm^2/Vs respectively. The three new polymers show good stability, with high temperature annealing showing an increase in the crystallinity of the polymers which corresponds directly to charge carrier mobility improvement as shown by X-ray diffraction, atomic force microscopy and photothermal deflection spectroscopy.

1. Introduction

Thin film organic field effect transistors (OFETs) based upon semiconducting polymers have tremendous potential for application in a wide variety of electronic applications. Solution processability allows for cheap large scale device fabrication through new techniques, such as inkjet printing, and the mechanical properties of plastics such as flexibility or stretchability allows for much more versatile devices.[1,2] Despite these advantages over conventional processing and form factors, the wide spread commercialization of organic semiconductor transistor devices is yet to be realized. A significant historical barrier to the progression of such materials is charge transport properties that are not sufficient for demanding applications, and the lack of a comprehensive understanding of how detailed structural design features of polymer organic frameworks relate to key device performance parameters such as hole and electron mobilities. In particular there is much interest in designing ambipolar materials that have balanced hole and electron mobilities.[3–5] Generally, p-type materials that transport holes are much more reported throughout the literature than n-type materials transporting electrons and n-type mobilities are often orders of magnitude lower for a given material.[6] Structural features such as low-lying LUMO levels for electron injection, efficient LUMO delocalization along the polymer backbone and strong intermolecular association facilitating overlap of adjacent orbitals are known to be desirable features for n-type mobility.[7–9]

Isoindigo is a well-known structural motif for the design of such OFET materials. Its electron-deficient core as well as its off axis dipole moment promotes intermolecular interactions and ambient stability is imparted through the generally low-lying HOMO levels.[10–15] The pigment unit is comprised of an aromatic donor group that is fused to a ketopyrrole core, and the nature of these aromatic groups can influence a variety of the polymer's properties.[16] We previously reported the synthesis of a thiophene flanked isoindigo (iIT) polymer and its impressive ambipolar performance in OFET devices.[17] Thiophene is known to be an excellent building block for organic semiconducting polymers and small molecules.[18–20] The combination of efficient conjugation, high polarizability and peripheral ring positions that are readily synthetically modified gives a unit with

---

I. Meager, Dr. B. C. Schroeder, Dr. C. B. Nielsen,
Dr. M. Planells, Dr. H. Bronstein, Dr. J. W. Rumer,
Dr. D. I. James, Dr. R. S. Ashraf, Prof. I. McCulloch
Department of Chemistry and Centre
for Plastic Electronics
Imperial College London
London, SW7 2AZ, UK
E-mail: i.meager11@imperial.ac.uk

M. Nikolka, A. Sadhanala, Prof. H. Sirringhaus
Cavendish Laboratory
University of Cambridge
J. J. Thompson Avenue
Cambridge, CB3 0HE, UK

Dr. H. Bronstein
Department of Chemistry
University College London
London, WC1H 0AJT, UK

Dr. P. Hayoz, Dr. J.-C. Flores
BASF Schweiz AG
4002, Basel, Switzerland

DOI: 10.1002/adfm.201402307

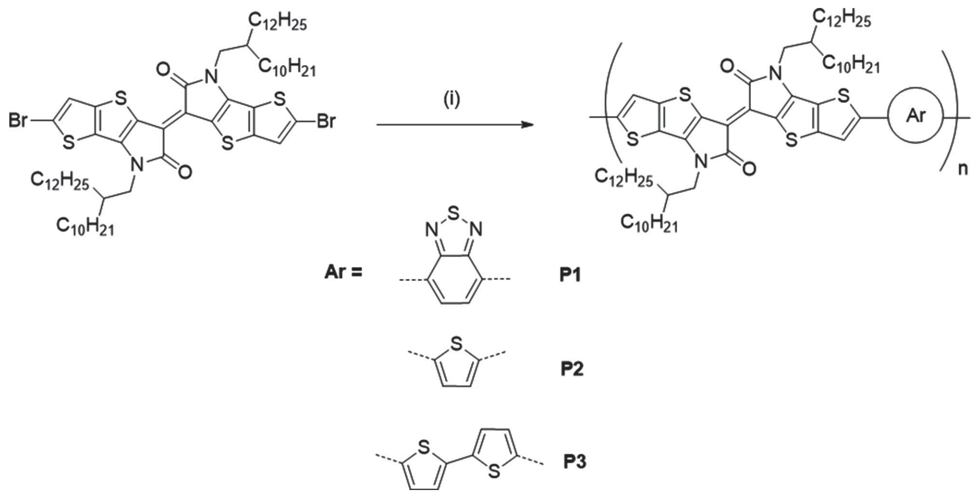

Figure 1. Copolymerisation of a dibrominated **iITT** monomer with benzothiadiazole, thiophene and bithiophene to afford polymers **P1**, **P2**, and **P3** respectively. Reagents and conditions: i) **P1** iITTBr$_2$, BT(Bpin)$_2$, PhMe, K$_2$CO$_3$, Aliquat 336, 120 °C 3 days. **P2** iITTBr$_2$, T(SnMe$_3$)$_2$, Pd$_2$(dba)$_3$, P(*o*Tol)$_3$, μW. **P3** iITTBr$_2$, 2T(SnMe$_3$)$_2$, Pd$_2$(dba)$_3$, P(*o*Tol)$_3$, μW.

very versatile properties. In comparison, thienothiophene contains two thiophene rings fused together, with three isomeric structures depending on the orientation of one thiophene ring relative to the second. When the thieno[3,2-*b*]thiophene isomer is incorporated into polymers, linked in the *2* and *5* positions, the fused nature has been shown to give an increased coplanarity along backbones, giving greater π-orbital overlap which can be beneficial for charge transport properties.[21–26]

With improvements having previously been demonstrated by the substitution of thiophene for thieno[3,2-*b*]thiophene in diketopyrrolopyrrole polymers, it was of interest to investigate the effect that the introduction of thieno[3,2-*b*]thiophene flanking units would have on the performance of isoindigo based copolymers. Hence we report the synthesis, characterisation and OFET performance of a new series of thieno[3,2-*b*]-thiophene based isoindigo (iITT) polymers (**Figure 1**) by copolymerization of the iITT monomer with benzothiadiazole, thiophene and bithiophene to exert varying degrees of control over the polymer's morphological features, energy level alignments and charge transport properties.

2. Results and Discussion

2.1. Polymer Synthesis and Properties

Figure 2 shows the synthesis of the new iITT monomer which was synthesised using a method analogous to the previously reported thiophene based isoindigo and is the first example of a conjugated six fused ring isoindigo system. 3-bromo-thieno[3,2-*b*]thiophene was asymmetrically synthesized from thieno[3,2-*b*]-thiophene, the branched 2-decyltetradecyl (C$_{10}$C$_{12}$) amine was attached at the *3*-position using a copper catalyzed Ullmann coupling. Once attached, the amine functionality was reacted with oxalyl chloride which forms the pyrrole dicarbonyl ring at the thieno[3,2-*b*]-thiophene *2*-position. The dicarbonyl unit was dimerised using Lawesson's reagent to give the iITT core which was subsequently brominated to give the final monomer. Full synthetic details and reaction schemes are included in the Supporting Information (SI).

Once synthesized, the dibrominated iITT monomer was copolymerised with a trio of monomer units. Benzothiadiazole (BT) was employed due to its electron withdrawing nature providing the basis for polymer molecular orbital hybridization leading to a low band gap, as well as the dipolar and sterically exposed nature of the BT unit facilitating short intermolecular contacts. Thiophene and 2,2′-bithiophene were chosen to function as conjugated, coplanar spacer groups, and are often incorporated into high performing charge transport materials. All three polymers were synthesised by palladium catalysed cross coupling; **P1** (benzothiadiazole, BT) using Suzuki coupling methods whilst **P2** (thiophene, T) and **P3** (bithiophene, 2T) were synthesised using Stille coupling. Following polymerization, catalytic impurities and lower molecular weight oligomers were removed by Soxhlet extraction in methanol, acetone and hexane. The desired polymeric materials were

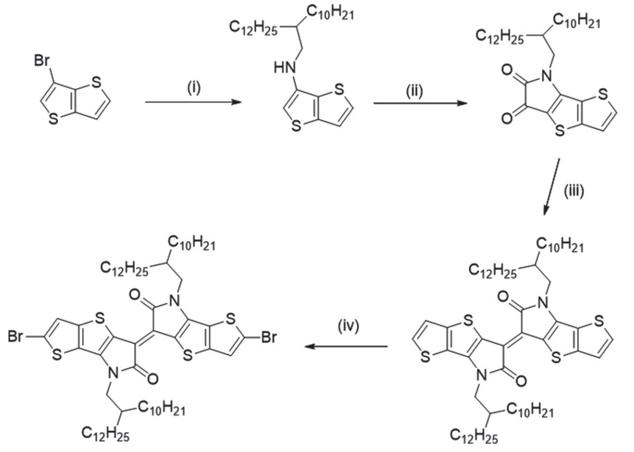

Figure 2. Synthesis of new dibrominated **iITT** monomer unit. Reagents and conditions: i) 2-decyltetradecyl amine, Cu, CuI, K$_2$PO$_4$, dimethyl aminoethanol, 80 °C, ii) oxalyl chloride, TEA, DCM, –10 °C, iii) Lawesson's Reagent, *o*-xylene, 60 °C, iv) NBS, THF, –10 °C.

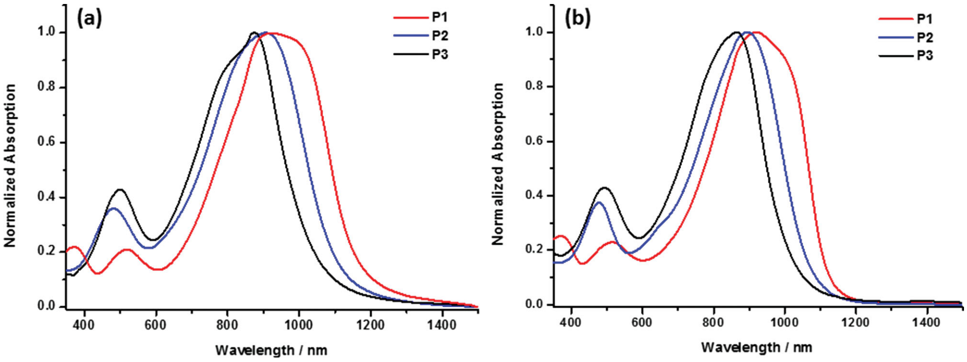

Figure 3. a) Thin film (spun from chlorobenzene 5 mg/mL) and b) solution UV–Vis absorption spectra for polymers **P1–P3**.

then isolated by Soxhlet extraction in chloroform and further purified using recycling gel permeation chromatography in chlorobenzene.[27] Each polymer was obtained in comparable molecular weights (M_n) ranging from 17 – 30 kDa with narrow polydispersity indexes (PDI) around 2. They show good solubility in common chlorinated solvents such as chloroform and chlorobenzene.

Polymers **P1–P3** all show broad absorption profiles (**Figure 3** and **Table 1**) with absorption maxima shifted towards the infra-red region of the spectrum. **P1** with benzothiadiazole as the comonomer unit shows the narrowest optical band gap (1.05 eV). The electron withdrawing BT comonomer unit lowers both the HOMO and LUMO energy level, however there is a larger electron density contribution from the thiadiazole unit to the LUMO as shown by density functional theory (DFT) calculations (Figure 5) resulting in a greater stabilization of the LUMO and an overall narrowing of the band gap. **P1** also has the most red-shifted thin film absorption profile as shown by UV–Vis with a maximum in the solid state at 926 nm and a slightly blue shifted absorption maximum in solution at 914 nm. In comparison, **P2** (thiophene) polymer has a more electron rich comonomer units which raises both the HOMO and LUMO levels. The LUMO is raised by a greater amount resulting in a slightly wider band gap of 1.13 eV. By adding an extra thiophene unit in the **P3** comonomer the polymer intramolecular charge transfer character is reduced which results in a wider band gap and blue-shifted absorption profile of **P3** relative to **P2**. Compared to **P1**, Both **P2** and **P3** have slightly less red-shifted thin film absorption profiles with **P2** showing an absorption maximum in the solid state at 909 nm and in solution at 897 nm. **P3** is the least red-shifted of the series with a maximum at 875 nm as a solid and 864 nm in solution.

2.2. OFET Device Properties and Characterization

Top-gate/bottom contact thin film OFET devices based on **P1–P3** were fabricated to evaluate the charge transport characteristics of the new isoindigo polymers. **Figure 4** shows typical transfer characteristics recorded at $V_D = -60$ V for the polymers **P1–P3** annealed for 1 h at 100 °C, 200 °C, and 300 °C in an inert atmosphere. A high maximum annealing temperature of 300 °C was achievable as differential scanning calorimetry (DSC) showed polymers **P1–P3** to be stable up to temperatures of 350 °C with no observable thermal transitions (see Supporting Information). Average charge carrier mobilities and threshold voltages were determined from the square root of the saturation transfer curve and are summarized in **Table 2**. The transfer characteristics of polymers **P1–P3** generally exhibit good ambipolar charge transport properties, with improvements observed at high temperature annealing. **P1** can be seen to have higher electron mobilities whilst **P3** has higher hole mobilities and **P2** has equally matched electron and hole mobilities. For all three polymers, an increase in overall current and charge carrier mobility with annealing temperature is observed; across the series there is a similar large boost in electron and hole currents when the annealing temperature is increased from 100 °C to 200 °C whilst a further increase in annealing temperature from 200 °C to 300 °C yields only minor improvements in currents. Similar mobility improvements with high temperature annealing have been observed in comparable diketopyrrolopyrrole (DPP) polymers[25,28] Overall the best performances could be obtained for the polymer **P1** with benozthiadiazole comonomer, giving average hole mobilities that show an increase from 0.1 cm^2/Vs at 100 °C to 0.3 cm^2/Vs at 200 °C and 0.4 cm^2/Vs at 300 °C. Electron mobilities for **P1**,

Table 1. Physical and optical properties of polymers **P1** – **P3**.

Polymer	M_n/M_w [kDa]a)	PDIa)	λ_{max} [nm]b)		HOMO		LUMO [eV]		Eg [eV]	
			Film	Solution	PESAc)	Calc.d)	UV–Vise)	Calc.d)	Observed	Calc.d)
P1	17/27	1.6	926	914	–4.9	–4.7	–3.9	–3.5	1.05	1.17
P2	30/67	2.3	909	897	–4.8	–4.6	–3.7	–3.3	1.13	1.31
P3	20/41	2.1	875	864	–4.8	–4.6	–3.6	–3.2	1.19	1.33

a)Determined by GPC (Chlorobenzene 80 °C) against polystyrene standards; b)Determined from UV–Vis absorption spectra; c)Determined by photoelectron spectroscopy in air (UV-PESA); d)Calculated by DFT/TD-DFT with a B3LYP/6–31g* basis set; e)Determined from absorption onset in thin film UV–Vis spectra.

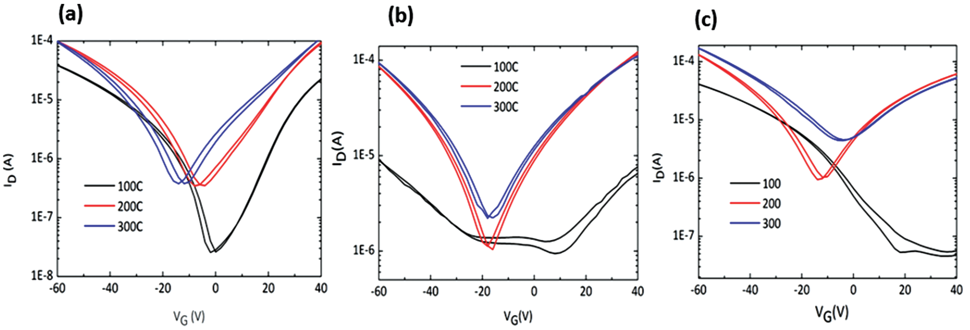

Figure 4. Transfer characteristics of a) **P1**, b) **P2**, and c) **P3** Top-Gate/Bottom-Contact OFET devices (L = 20 μm, W = 1 mm) annealed at different temperatures and measured at V_D = –60 V.

which are on the same order of magnitude, go from 0.2 cm^2/Vs at 100 °C to 0.5 cm^2/Vs at 200 °C and 0.7 cm^2/Vs at 300 °C. Superior electron mobility for polymers containing a BT unit have been reported several times previously in the literature and it is believed that the electron-deficient nature of the unit lowers the LUMO energy by a sufficient amount as to enhance electron injection from the high work function electrode.[29] Additionally, the planar structure of the polymer backbone (**Figure 5**.) benefits charge transfer through interchain hopping. When compared to the equivalent thiophene isoindigo *co*-benzothiadiazole polymer the devices can be seen to have significantly improved hole and electron mobilities whilst retaining their ambipolar nature.[17] Replacing the benzothiadiazole comonomer with thiophene (**P2**), interestingly results in mobilities that are balanced for holes and electrons with values of 0.2 cm^2/Vs at 200 °C and 300 °C observed for both. Polymerisation with a bithiophene comonomer in **P3** affords devices with improved hole transport. Maximum mobilities are observed at 200 °C and 300 °C for both holes and electrons, with values of 0.4 cm^2/Vs and 0.1 cm^2/Vs respectively.

The polymer backbone co-planarities between adjacent aromatic units and long axis linearities, as approximated by DFT calculations modelling gas phase co-trimer units in a vacuum with a B3LYP/6–31g* basis set are shown in Figure 5. Polymer **P1** with the benzothiadiazole comonomer shows very little backbone twist and is significantly more planar than the **P2** and **P3**. Both **P1** and **P3** show strongly linear backbones whereas the linearity in **P2**, with the thiophene comonomer, is noticeably less. All three polymers have good delocalization of both HOMO and LUMO energy levels along the polymer backbone, with delocalization onto both the donor and acceptor repeating units, which are known to be important factors for hole and electron transport respectively.[4,30,31]

Table 2. Top gate/bottom contact OFET devices characteristics for polymers **P1–P3**.

Polymer	T_{anneal} [°C][a)]	μ_e [cm^2/Vs][b)]	μ_h [cm^2/Vs][b)]	V_{th} (electrons) [V][b)]	V_{th} (holes) [V][b)]
P1	100	0.2	0.1	14	–10
	200	0.5	0.3	12	–13
	300	0.7	0.4	13	–20
P2	100	0.01	0.01	7	–32
	200	0.2	0.2	–18	–24
	300	0.2	0.2	–24	–22
P3	100	-	0.01	n/a	3
	200	0.1	0.4	–18	–25
	300	0.1	0.4	–11	–21

[a)] Annealed for 1 h in an inert atmosphere; [b)] Average values determined from the square root of the saturation transfer curve.

OFET mobilities were observed to increase significantly with high temperature annealing at 100 °C, 200 °C, and 300 °C for 1 h in an inert atmosphere. To determine the origin of this improvement the polymer films were probed by out of plane X-ray diffraction scattering (XRD) and atomic force microscopy (AFM). For each of the three copolymers, a large increase in crystallinity was observed at higher annealing temperatures as shown by XRD (see **Figure 6**) which is in good agreement with the improvement in charge carrier mobility reported in Table 2 and Figure 4. The large enhancement in crystallinity with annealing is indicated by an increased intensity of the first order (100) and second order (200) lamellar stacking peaks, at $2\theta = 4.1°$ and $2\theta = 8.2°$ respectively, in all three polymer films corresponding to a lamellar stacking distance of 21.5 Å. The intensities of these peaks are slightly less in the case of **P2** which additionally shows an increasing broad π–π stacking peak at $2\theta = 25.0°$ that corresponds to a stacking distance of 3.6 Å. The most crystalline systems **P1** and **P3** also show a small third order (300) diffraction peak at $2\theta = 12.3°$ that is not present in the as-cast films and only becomes apparent at higher annealing temperatures. Moreover, the specular diffraction scatterings provide further morphological detail in relation to the orientation of the polymer chains relative to the substrate. Benzothiadiazole and bithiophene comonomer units, used in **P1** and **P3** respectively, show a predominantly edge-on orientation. The thiophene comonomer unit, used in **P2**, shows an observably different orientation to the substrate with a larger face-on contribution as seen by the strong π–π stacking peak. Such an enhancement in face-on orientation with the introduction of a thiophene spacer is in agreement with previous studies on similar DPP polymers.[32]

AFM images of the three polymers across the range of annealing temperatures are shown in Figure S9 (Supporting Information). For polymers **P1–P3** it is clear there is no

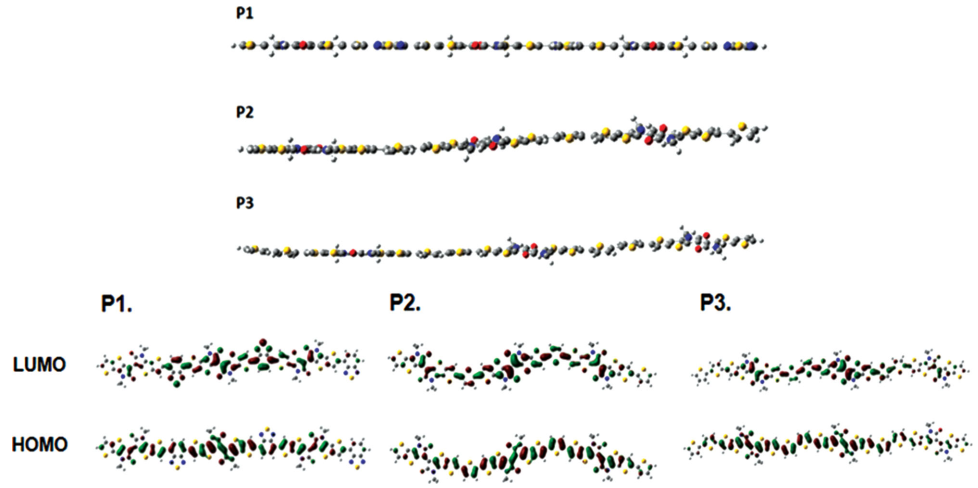

Figure 5. HOMO and LUMO molecular orbital distributions for polymers **P1–P3** as calculated using DFT with a B3LYP/6–31g* basis set.

dramatic observable change in surface morphology/roughness as the films progress to higher annealing temperatures. Both **P1** and **P3** show very similar surface roughness, both demonstrating only small changes at higher annealing temperatures. **P2** shows a slightly more pronounced change at higher temperatures, going from the as-cast polymer film to 300 °C sees the polymer films becoming noticeably coarser. Whilst it is difficult to strongly relate the surface of polymer films to their bulk behavior as a solid, this is likely a result of the change in polymer chain orientation relative to the plane of the substrate as observed by XRD with the appearance of a strong π–π stacking peak at high temperatures. Photothermal deflection spectroscopy (PDS) measurements were performed on polymer films of **P1**, **P2**, and **P3** annealed at 200 °C, to investigate the effects of energetic disorder on charge transport and thus, complement the results on structural disorder obtained from XRD and are shown in **Figure 7**. PDS accurately measures the absorption tail in the extended region

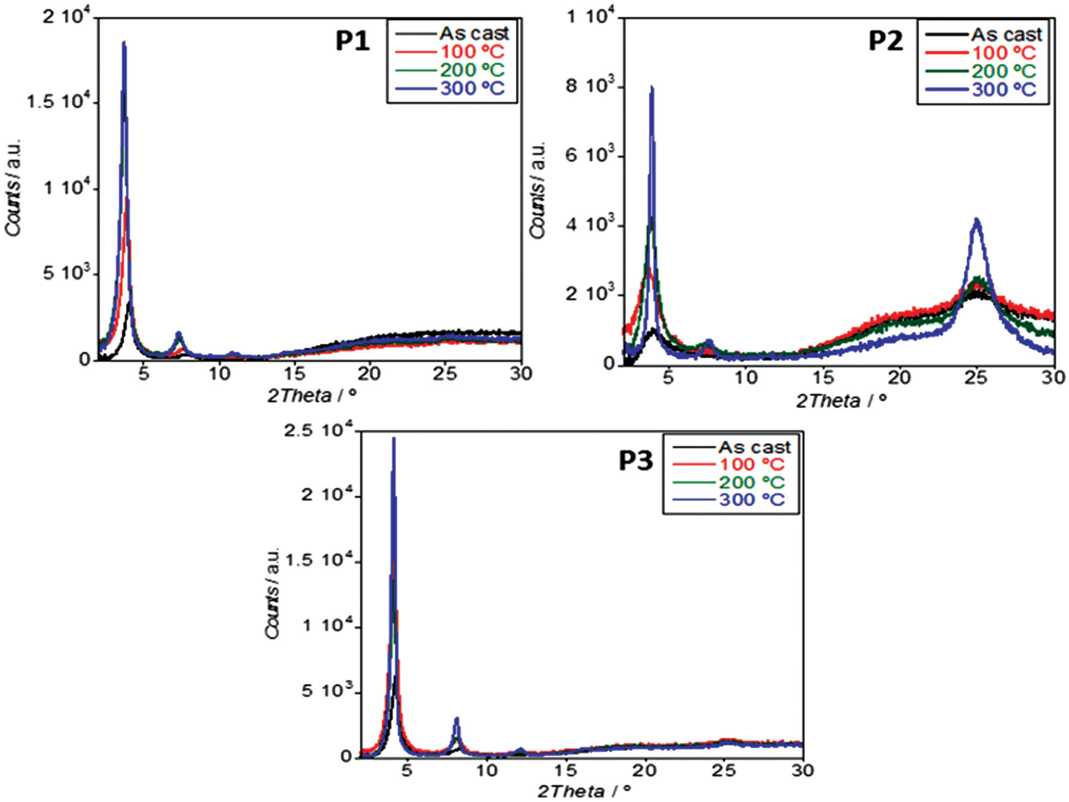

Figure 6. XRD diffractograms of **P1–P3** as cast and at annealing temperatures of 100 °C, 200 °C, and 300 °C.

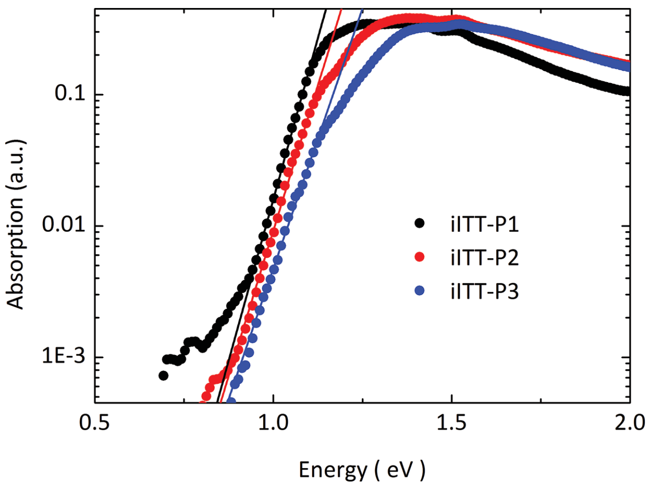

Figure 7. Normalized Photothermal Deflection Spectroscopy (PDS) spectra of **P1**, **P2**, and **P3**. Fits used for the extraction of the Urbach energy are shown as solid lines.

below the band edge, where absorption decreases exponentially with energy, full details are included in the Supporting Information. From the sharpness of the absorption tail, the Urbach energy can be extracted as a measure of energetic disorder in the film. For the corresponding iITT- polymers, similar Urbach energies of 44 meV for **P1**, 49 meV for **P2** and 55 meV for **P3** could be extracted, where the error in determining the Urbach energy is estimated to be 5 meV for each of the polymers. These values are comparable to other highly crystalline systems such as PBTTT which show similar charge carrier mobilities as well as Urbach energies.[33,34] Within the error range, the extracted Urbach energies are furthermore, in good agreement with the trend in mobility reported across the polymer series in Table 2.

3. Conclusion

A new thieno[3,2-*b*]thiophene based isoindigo monomer unit and copolymers are presented. Copolymers with benzothiadiazole, thiophene and bithiophene are synthesized, characterized and their charge transport properties analyzed, each polymer is stable to high temperature annealing and show red shifted absorption profiles with absorption maxima around 900 nm. The introduction of the thieno[3,2-*b*]thiophene unit to the isoindigo structure demonstrates a design strategy towards high charge transport, ambipolar characteristics in thin film OFET devices with hole mobilities up to 0.4 cm^2/Vs and electron mobilities up to 0.7 cm^2/Vs observed. Through comonomer variation a simple parameter is used effectively to tune the type of transport and demonstrate the versatility of the iITT unit with benzothiadiazole comonomer showing predominantly electron transport, bithiophene predominantly hole transport and thiophene showing balanced electron and hole transport. Thermal annfealing of the OFET devices is found to improve the charge transport characteristics of the polymer materials with a direct correlation to crystallinity of the polymer films observed as probed by X-ray diffraction studies.

Supporting Information

Supporting Information is available from the Wiley Online Library or from the author.

Acknowledgements

The authors are grateful to Dr. Scott Watkins (CSIRO) for PESA measurements. This work was carried out primarily with funding from The Leventis Foundation and BASF. M.N. and H.S. acknowledge funding support from the Technology Strategy Board (PORSCHED project, 16252–119144). B.C.S would like to acknowledge financial support from The Luxembourg research fund.

Received: July 12, 2014
Revised: August 12, 2014
Published online: September 10, 2014

---

[1] T. Sekitani, U. Zschieschang, H. Klauk, T. Someya, *Nat. Mater.* **2010**, *9*, 1015.
[2] S. J. Benight, C. Wang, J. B. H. Tok, Z. Bao, *Prog. Polym. Sci.* **2013**, *38*, 1961.
[3] Y. Zhao, Y. Guo, Y. Liu, *Adv. Mater.* **2013**, *25*, 5372.
[4] I. Osaka, T. Abe, H. Mori, M. Saito, N. Takemura, T. Koganezawa, K. Takimiya, *J. Mater. Chem. C* **2014**, *2*, 2307.
[5] B. Sun, W. Hong, Z. Yan, H. Aziz, Y. Li, *Adv. Mater.* **2014**, *26*, 2636.
[6] C. B. Nielsen, M. Turbiez, I. McCulloch, *Adv. Mater.* **2012**, *25*, 1859.
[7] J. E. Anthony, A. Facchetti, M. Heeney, S. R. Marder, X. Zhan, *Adv. Mater.* **2010**, *22*, 3876.
[8] A. J. Kronemeijer, E. Gili, M. Shahid, J. Rivnay, A. Salleo, M. Heeney, H. Sirringhaus, *Adv. Mater.* **2012**, *24*, 1558.
[9] S. Holliday, J. E. Donaghey, I. McCulloch, *Chem. Mater.* **2013**, *26*, 647.
[10] T. Lei, J.-H. Dou, Z.-J. Ma, C.-H. Yao, C.-J. Liu, J.-Y. Wang, J. Pei, *J. Am. Chem. Soc.* **2012**, *134*, 20025.
[11] T. Lei, J.-Y. Wang, J. Pei, *Acc. Chem. Res.* **2013**, *47*, 1117.
[12] R. Stalder, J. Mei, K. R. Graham, L. A. Estrada, J. R. Reynolds, *Chem. Mater.* **2013**, *26*, 664.
[13] T. Lei, Y. Cao, Y. Fan, C.-J. Liu, S.-C. Yuan, J. Pei, *J. Am. Chem. Soc.* **2011**, *133*, 6099.
[14] T. Lei, Y. Cao, X. Zhou, Y. Peng, J. Bian, J. Pei, *Chem. Mater.* **2012**, *24*, 1762.
[15] P. Deng, Q. Zhang, *Polym. Chem.* **2014**, *5*, 3298.
[16] J. W. Rumer, B. C. Schroeder, C. B. Nielsen, R. S. Ashraf, D. Beatrup, H. Bronstein, S. J. Cryer, J. E. Donaghey, S. Holliday, M. Hurhangee, D. I. James, S. Lim, I. Meager, W. Zhang, I. McCulloch, *Thin Solid Films* **2014**, *560*, 82.
[17] R. S. Ashraf, A. J. Kronemeijer, D. I. James, H. Sirringhaus, I. McCulloch, *Chem. Commun.* **2012**, *48*, 3939.
[18] T.-A. Chen, X. Wu, R. D. Rieke, *J. Am. Chem. Soc.* **1995**, *117*, 233.
[19] N. Stutzmann, R. H. Friend, H. Sirringhaus, *Science* **2003**, *299*, 1881.
[20] J. C. Bijleveld, A. P. Zoombelt, S. G. J. Mathijssen, M. M. Wienk, M. Turbiez, D. M. de Leeuw, R. A. J. Janssen, *J. Am. Chem. Soc.* **2009**, *131*, 16616.
[21] H. Bronstein, Z. Chen, R. S. Ashraf, W. Zhang, J. Du, J. R. Durrant, P. S. Tuladhar, K. Song, S. E. Watkins, Y. Geerts, M. M. Wienk, R. A. J. Janssen, T. Anthopoulos, H. Sirringhaus, M. Heeney, I. McCulloch, *J. Am. Chem. Soc.* **2011**, *133*, 3272.

[22] H. Bronstein, E. Collado-Fregoso, A. Hadipour, Y. W. Soon, Z. Huang, S. D. Dimitrov, R. S. Ashraf, B. P. Rand, S. E. Watkins, P. S. Tuladhar, I. Meager, J. R. Durrant, I. McCulloch, *Adv. Funct. Mater.* **2013**, *23*, 5647.

[23] I. Meager, R. S. Ashraf, S. Rossbauer, H. Bronstein, J. E. Donaghey, J. Marshall, B. C. Schroeder, M. Heeney, T. D. Anthopoulos, I. McCulloch, *Macromolecules* **2013**, *46*, 5961.

[24] I. Meager, R. S. Ashraf, S. Mollinger, B. C. Schroeder, H. Bronstein, D. Beatrup, M. S. Vezie, T. Kirchartz, A. Salleo, J. Nelson, I. McCulloch, *J. Am. Chem. Soc.* **2013**, *135*, 11537.

[25] Y. Li, S. P. Singh, P. Sonar, *Adv. Mater.* **2010**, *22*, 4862.

[26] Z. Chen, M. J. Lee, R. Shahid Ashraf, Y. Gu, S. Albert-Seifried, M. Meedom Nielsen, B. Schroeder, T. D. Anthopoulos, M. Heeney, I. McCulloch, H. Sirringhaus, *Adv. Mater.* **2012**, *24*, 647.

[27] R. S. Ashraf, B. C. Schroeder, H. A. Bronstein, Z. Huang, S. Thomas, R. J. Kline, C. J. Brabec, P. Rannou, T. D. Anthopoulos, J. R. Durrant, I. McCulloch, *Adv. Mater.* **2013**, *25*, 2029.

[28] P. Sonar, S. P. Singh, Y. Li, M. S. Soh, A. Dodabalapur, *Adv. Mater.* **2010**, *22*, 5409.

[29] J. Smith, R. Hamilton, I. McCulloch, N. Stingelin-Stutzmann, M. Heeney, D. D. C. Bradley, T. D. Anthopoulos, *J. Mater. Chem.* **2010**, *20*, 2562.

[30] Y. Olivier, D. Niedzialek, V. Lemaur, W. Pisula, K. Müllen, U. Koldemir, J. R. Reynolds, R. Lazzaroni, J. Cornil, D. Beljonne, *Adv. Mater.* **2014**, *26*, 2119.

[31] Y. Yamaguchi, K. Ogawa, K. Nakayama, Y. Ohba, H. Katagiri, *J. Am. Chem. Soc.* **2013**, *135*, 19095.

[32] X. Zhang, L. J. Richter, D. M. DeLongchamp, R. J. Kline, M. R. Hammond, I. McCulloch, M. Heeney, R. S. Ashraf, J. N. Smith, T. D. Anthopoulos, B. C. Schroeder, Y. H. Geerts, D. A. Fischer, M. F. Toney, *J. Am. Chem. Soc.* **2011**, *133*, 15073.

[33] I. McCulloch, M. Heeney, C. Bailey, K. Genevicius, I. MacDonald, M. Shkunov, D. Sparrowe, S. Tierney, R. Wagner, W. Zhang, M. L. Chabinyc, R. J. Kline, M. D. McGehee, M. F. Toney, *Nat. Mater.* **2006**, *5*, 328.

[34] A. J. Kronemeijer, V. Pecunia, D. Venkateshvaran, M. Nikolka, A. Sadhanala, J. Moriarty, M. Szumilo, H. Sirringhaus, *Adv. Mater.* **2014**, *26*, 728.